EDGE DETECTION IN TEXTURES

Larry S. Davis
Amar Mitiche

Computer Sciences Department
The University of Texas at Austin
Austin, Texas 78712

TR-111 October 1979

This research was supported in part by funds derived from the Air Force Office of Scientific Research under contract F49620-79-C-0043

1. Introduction

Detecting edges is an important first step in the solution of many image analysis tasks. Edges are used primarily to aid in the segmentation of an image into meaningful regions, but are also extensively used to compute relatively local measures of textural variation (which, of course, can subsequently be used for segmentation purposes). Although there has been a considerable amount of research concerning quantitative models for edge detection (e.g., Nahi [1], Modestino and Fries [2], Shanmugan et al [3], Cooper and Elliot [4]), very little work has been devoted to developing such models for images described by texture models. This paper addresses the problem of detecting edges in what are called macro-textures, i.e., cellular textures where the cells, or texture elements, are relatively large (at least several pixels in diameter).

Once edges are detected in texture regions, they can be used to define texture descriptors in a variety of ways. For example, one can compute "edge per unit area" (Rosenfeld [5]). More generally, one can compute first-order statistics of edge properties [6,7], such as orientation, contrast, fuzziness, etc., or higher-order statistics which can measure the spatial arrangement of edges in the texture. Such statistics can be computed from generalized cooccurrence matrices (Davis et al [8,9]) which count the number of times that specific pairs of edges occur in specific relative spatial positions. Clearly, the utility of such tools depends on the reliability with which edges can be detected in textures.

This paper is organized as follows: Section 2 contains a description

of the image texture models which will be considered. These models are one-dimensional, since the edge-detection procedures, described in Section 3, are one-dimensional. Section 4 contains derivations of the expected value and variance of the edge operator described in Section 3 and describes optimal edge detection procedures based on that analysis. Finally, Section 5 contains conclusions and a summary.

2. Texture Models

There are a large number of formal image texture models which have been proposed and studied during the past few years. These can be broadly classified as pixel-based and region-based models (Ahuja [10]). All of these models treat textures as a two-dimensional phenomena, which is appropriate for many applications (e.g., some medical applications, geographical applications). However, for other applications, regarding textures in this way is inappropriate; one should, instead, model the texture as a surface in space with certain reflectance properties. An image of such a texture is then determined by the spatial disposition of the surface and the viewer, the frequency response of the viewer, and the positions of all light sources. Horn [11] should be consulted for an introduction to this branch of image science. Such models will not be considered in this paper.

Pixel-based models are ordinarily time-series models or random field models. Time-series models have been investigated by McCormick and Jayaramamurthy [12], and by Tou et al [13]. Random field models are discussed in Wong [14], and Pratt et al [15]. For more references, see [16-17].

This paper will be concerned with region-based texture models. In particular, we will consider one-dimensional models which are related to two-dimensional cell structure models. Cell structure models describe textures as mosaics, and can be generated by the following two-step process:

1) A planar region is tessellated into cells, ordinarily convex.

2) Each cell is independently assigned one of m colors, $c_1,\ldots,c_m$, using a fixed set of probabilities, $p_1,\ldots,p_m$.

This process partitions the original region into subregions, which are the unions of cells of constant color. If A is the original region, then $A_1,\ldots,A_m$ are the subregions. Note that the simple colors can be replaced by more complex coloring processes, e.g., the grey levels in a cell can be chosen according to a given distribution, d, which is itself chosen from a set of distributions, D, according to the given probability vector, P. Ahuja [10] contains an extensive survey of such models.

We will consider a similar class of one-dimensional models. A texture model is an ordered pair <P,C> where

1) P is a cell width model, which successively drops intervals along a line, and

2) C is a coloring model, consisting of coloring processes, $c_1,\ldots,c_m$, and probabilities, $p_1,\ldots,p_m$. As P produces cells, C colors the cells.

If we let w be the random variable corresponding to cell width, then the following are examples of cell width models:

1) Constant cell width model

$$P_c(w) = \begin{cases} 1 & w=b \\ 0 & w\neq b \end{cases}$$

2) Uniform cell width model

$$P_u(w) = \begin{cases} 1/b & 0 \leq w \leq b \\ 0 & w > b \end{cases}$$

3) Exponential cell width model

$$P_e(w) = \lambda \exp[\lambda w].$$

To simplify the analysis, we assume that there are only two coloring processes, c_1 and c_2. Therefore, there is only one relevant probability for choosing cell colors, which will be denoted by p. Each coloring process colors a cell by choosing the intensity of each point in that cell independently from a normal distribution of intensities. The distributions are denoted $N(m_i,v_i)$, i=1,2, with mean m_i and variance v_i.

Notice that given a one-dimensional cell structure model, <P,C>, one can derive a one-dimensional component structure model, where a component is a contiguous set of identically colored cells. For example, for the cell model $<P_c,C>$ the corresponding component model has components whose lengths are distributed geometrically. Of course, in a component model, the various colors alternate, since by definition two adjacent components must have different colors. The component model is required to determine the prior probabilities of various types of pixels (see Section 4).

3. A One-Dimensional Edge-Detector

In this section we will describe a simple, one-dimensional edge detection procedure. There are a variety of reasons for considering one-dimensional edge detectors:

1) Computational efficiency on conventional, sequential computers. Since we are interested in detecting edges for the purpose of describing texture, it is important that the edge detection process be made as efficient as possible.

2) Suitability for implementation on special-purpose image processing hardware. There has been a significant amount of research and development of image processing hardware over the past few years (CLIP [18], PICAP [19]). One-dimensional edge detectors can be easily implemented on, for example, series-parallel machines, where a row of processors "scan" and process the image one row at a time.

3) Mathematical tractability. Direct analysis of two-dimensional edge detectors is complicated by many factors, including the mathematical complexity of most two-dimensional cellular texture models and the greater variety of edge-like features in two dimensions.

The class of edge operators which we have considered is based on differences of averages between adjacent, symmetric one-dimensional image neighborhoods. Specifically, let f be a one-dimensional image function. Then the edge operator is:

$$e_k(i) = (1/k) \sum_{j=1}^{k} (f(i-j)-f(i+j))$$

$$= (1/k)\ (LS(i)-RS(i))$$

where

$$LS(i) = \sum_{j=1}^{k} f(i-j) \quad \text{and}$$

$$RS(i) = \sum_{j=1}^{k} f(i+j)$$

By noticing that

$$e_k(i+1) = (1/k)\ [LS(i)-f(i-k) + f(i)-RS(i) + f(i+1)-f(i+k+1)]$$

we see that e_k can be computed in a constant number of operations per picture point, independent of k, on a conventional sequential computer.

The operator e_k is used to detect edges by the following three step process:

1) Compute $e_k(i)$ for all points i.

2) Discard all i with $|e_k(i)| < t$. This thresholding step is intended to discriminate between points which are edges of texture elements and points which are in the interior of texture elements, but far from edges.

3) Discard all i with $|e_k(i)| < |e_k(i+j)|$, $|j| < d$. This non-maxima suppression step is intended to discriminate between points which are edges and points which are interior to texture elements, but are close to edges.

Step 3 is crucial since e_k gives high response not just at edges, but also near edges, so that thresholding alone would result in a cluster of detections about each true edge point. The above procedure involves three classes of texture pixels:

1) edge pixels, which are pixels located directly at the edges between texture elements;

2) near-edge pixels, which are located within distance d of an

edge pixel and are discarded by the non-maxima suppression step; and

3) interior pixels, which are located distances greater than d from the nearest edge pixel, and are ordinarily eliminated by the thresholding step (but may be eliminated due to proximity to above threshold, near-edge pixels).

Optimizing the above edge detection procedure involves choosing k, t and d in order to minimize the probability of error--i.e., minimizing the frequency of discarding edge points, and not discarding near-edge and interior pixels. This paper considers the edge-interior discrimination problem only. Therefore, we will be concerned with choosing values for k and t only. The complete edge detector, including the non-maxima suppression step, is discussed in Davis and Mitiche [20].

4. Analysis of e_k

In this section we will derive the expected value and variance of e_k at edges and at interior points. We will regard an interior point as a point whose distance from the nearest edge is greater than k. Expressions for the prior probabilities of edge and interior points are developed. Finally, by assuming that e_k is normally distributed at edges and interiors, a minimum error thresholding procedure for distinguishing between edge points and interior points is developed.

4.1 The expected value of e_k, $E[e_k]$

The definition of e_k was originally given for a discrete function f. If f is continuous, then we can redefine e_k as

$$e_k(i) = 1/k \left[\int_{-k}^{0} f(i+j)dj - \int_{0}^{k} f(i+j)dj \right]$$

Then, the expected value of e_k is

$$E[e_k(i)] = 1/k \left[\int_{-k}^{0} E[f(i+j)]dj - \int_{0}^{k} E[f(i+j)]dj \right]$$

If i is an interior point, then all points f(i+j), $-k \leq j \leq k$ are colored by the same process. Therefore, the expected values are all the same, and thus $E[e_k(i) | i \text{ is an interior point}] = 0$.

Now suppose that i is an edge point, and assume, without loss of generality, that the cell to the left of i, C_ℓ, is colored by process c_1, and that the cell to the right of i, C_r, is colored by by process c_2, and that $m_1 > m_2$. Let w_ℓ be the width of C_ℓ and w_r be the width of C_r (see Figure 1). We will also make the simplifying assumption that the points

to the left of C_ℓ (or the right of C_r) are individually colored with processes c_1 and c_2 with probabilities p and (1-p). For k much greater than w_ℓ or w_r, this assumption is not unreasonable. As w_ℓ or w_r approaches k, it is more likely that only one cell will be found to the left of C_ℓ or the right of C_r. However, large cells are ordinarily less likely than small cells. Letting $a = pm_1 + (1-p)m_2$, we can then write

$$E[e_k(i)] = 1/k \left[\left(\int_0^k (m_1 w_\ell + a(k-w_\ell)P(w_\ell)dw_\ell + \int_k^\infty m_1 k P(w_\ell)dw_\ell \right) \right.$$

$$\left. - \int_0^k (m_2 w_r + a(k-w_r)P(w_r)dw_r + \int_k^\infty m_2 k P(w_r)dw_r) \right]$$

Since w_ℓ and w_r are drawn from the same distribution, terms can be grouped to obtain

$$E[e_k(i)] = 1/k \left[\int_0^k (m_1-m_2)wP(w)dw + \int_k^\infty (m_1-m_2)kP(w)dw \right]$$

$$= 1/k \left[(m_1-m_2)w_0 - \int_k^\infty (m_1-m_2)wP(w)dw + \int_k^\infty (m_1-m_2)kP(w)dw \right]$$

$$= \frac{(m_1-m_2)}{k} \left[w_0 - \int_k^\infty (w-k)P(w)dw \right]$$

where

$$w_0 = \int_0^\infty wP(w)dw.$$

4.2 The variance of e_k

From the definition of e_k, we have

$$\text{Var}\,[e_k(i)] = \text{Var}\left[1/k \int_0^k f(i-j)-f(i+j)dj \right]$$

Suppose i is an interior point and is in a cell colored by c_1. Then

$$\text{Var}[e_k(i)] = (1/k^2)\, k\, 2v_1$$

$$= 2v_1/k$$

If i is an interior point and is in a cell colored by c_2, then $\text{Var}[e_k(i)] = 2v_2/k$.

Next we will consider the case of i, an edge point. Let

$$LS(i) = \int_0^k f(i-j)dj$$

$$RS(i) = \int_0^k f(i+j)dj$$

Then

$$e_k(i) = 1/k\ (LS(i)-RS(i))$$

We will derive expressions for Var[LS(i)] and Var[RS(i)]. There are two cases to consider:

1) w_ℓ or $w_r \geq k$

2) w_ℓ or $w_r < k$

If $w_\ell \geq k$, then the variance of LS(i) is kv_1. If $w_r \geq k$, then the variance of RS(i) is kv_2.

Next, suppose $w_\ell < k$. We will assume that of the $k-w_\ell$ pixels not in C_ℓ, ℓ_1 pixels are colored by process c_1 and $\ell_2 = (k-w_\ell)-\ell_1$ pixels are colored by process c_2, where ℓ_1 is a random variable described by a binomial distribution with parameter p and ℓ_2 is a random variable described by a binomial distribution with parameter (1-p).

In general, if y is the sum of a random number, n, of independent

experimental values of a random variable x, then

$$\mathrm{Var}[y] = E[n]\ \mathrm{Var}[x] + (E[x])^2\ \mathrm{Var}[n]$$

Thus, if w_ℓ is a fixed value less than k,

$$\mathrm{Var}[LS(i) \mid w_\ell < k] =$$

$$w_\ell v_1 + E[\ell_1] v_1 + m_1^2\ \mathrm{Var}[\ell_1]$$

$$+ E[\ell_2] v_2 + m_2^2\ \mathrm{Var}[\ell_2]$$

with

$$E[\ell_1] = (k - w_\ell) p$$

$$E[\ell_2] = (k - w_\ell)(1-p)$$

$$\mathrm{Var}[\ell_1] = \mathrm{Var}[\ell_2] = (k - w_\ell)\, p(1-p)$$

A similar expression can be obtained for RS(i).

Combining the cases $w_\ell \geq k$ and $w_\ell < k$, we can write

$$\mathrm{Var}[LS(i) \mid i \text{ an edge}] =$$

$$\frac{1}{k^2} \left[\int_k^\infty k v_1 P(w_\ell)\, dw_\ell \right.$$

$$+ \int_0^k (w_\ell v_1 + (k - w_\ell)(p v_1 + (1-p) v_2)$$

$$\left. + (k - w_\ell)\, p(1-p)(m_1^2 + m_2^2))\, P(w_\ell)\, dw_\ell \right]$$

Again, a similar expression is obtained for RS(i). Since

$$\mathrm{Var}[e_k(i)] = 1/k^2\ [\mathrm{Var}[LS(i)] + \mathrm{Var}[RS(i)]]$$

Since w_ℓ and w_r are drawn from the same distribution, we group terms and

finally obtain, for edge points,

$$\mathrm{Var}[e_k(i) \mid i \text{ is an edge}] =$$

$$1/k^2 \Big[k(v_1+v_2) \int_k^{\infty} P(w)dw$$

$$+ (v_1+v_2) \int_0^k wP(w)dw$$

$$+ 2(pv_1+(1-p)v_2) \int_0^k (k-w)P(w)dw$$

$$+ 2p(1-p)(m_1^2+m_2^2) \int_0^k (k-w)P(w)dw \Big]$$

For the exponential model with $p = .5$, for example, we find that

$$E[e_k(i) \mid i \text{ is an edge}] = \frac{(m_1-m_2)(1-e^{-\lambda k})}{\lambda k}$$

and

$$\mathrm{Var}[e_k(i) \mid i \text{ is an edge}] = \frac{(v_1+v_2)}{k} + \frac{m_1^2+m_2^2}{2k} \left(1 - \frac{1-e^{-\lambda k}}{\lambda k}\right)$$

Other simple expressions can be obtained for the constant and uniform models.

In order to derive a minimum error threshold for discriminating between edge and interior points using e_k, it is necessary to:

1) determine the prior probabilities of edge and interior points, and

2) specify a form for the distribution of e_k at edges and at interior points.

To compute the prior probabilities of edge and interior point, we must derive a component model from the cell width model. A component is a set of connected, identically colored cells. Let a c_1-component (c_2-component) be a component whose cells are colored by process c_1 (c_2). Then, the length of a component is defined to be the number of cells that compose it, and the width of a component is its actual measure.

In the following we will show how a component model can be derived from a cell model. As mentioned before, the cell coloring process is a Bernoulli process which selects coloring process c_1 with probability p and coloring process c_2 with probability (1-p). Therefore, the c_1-component and c_2-component lengths are random variables described by a geometric probability mass function. In the following analysis we will consider only c_1-components and simply refer to them as components. The same analysis will hold for c_2-components.

If n is the random variable that represents component length and $p_\ell(n)$ is the probability mass function for it, then

$$p_\ell(n) = (1-p)\, p^{n-1}$$

Now, if w and r are random variables that describe the cell width and the component width respectively, then r is the sum of a random number n of independent identically distributed experimental values of x:

$$r = \sum_{i=1}^{n} x_i$$

Expressions for the expected value and variance of r can be obtained in terms of the expected value and variance of n and w:

$$E[r] = E[n]\,E[w]$$

$$Var[r] = E[n]\,Var[w] + (E[w])^2\,Var[n]$$

If w is continuous and if f and g are the probability density functions for w and r, then

$$g^T(s) = p_\ell^T(f^T(s))$$

where f^T and g^T are the exponential transforms (s-transforms) of f and g respectively, and p_ℓ^T is the z-transform (discrete transform) of p_ℓ.

If w is discrete, then the above expression holds with f and g being the probability mass functions for w and r, and f^T and g^T being their respective z-transforms. By taking the inverse transforms one can obtain the distribution of component widths.

Examples

1. Constant distribution of cell width. For the constant cell width model, g is described by the geometric probability mass function

$$g(r) = \begin{cases} (1-p)\,p^{\frac{r}{b}-1} & \text{for } r = b,2b,3b,\ldots \\ 0 & \text{otherwise} \end{cases}$$

$$E[r] = b/(1-p)$$

$$Var[r] = b^2\,p/(1-p)^2$$

2. Exponential distribution of cell width. For the exponential model with parameter λ, g is described by the probability density function

$$g(r) = (1-p)\,\lambda\,\mathrm{Exp}(-(1-p)\lambda r)$$

Thus component widths are still exponentially distributed and

$$E[r] = 1/((1-p)\lambda)$$

3. Uniform distribution of cell width.

$$E[r] = b/(2(1-p))$$

$$\mathrm{Var}[r] = \frac{b/(4(1-p))}{(1/3 + p/(1-p))}$$

and

$$g(r) = e^{(p/b)r}\, g'(r)$$

where

$$g'(r) = (1-p)\left[\sum_{n=0}^{\infty} \frac{(-1)^n p^n e^{-np}}{b^{n+1}} \frac{(r-bn)^n}{\Gamma(n+1)} S_{bn}(r) - \frac{1}{e^p} \sum_{n=0}^{\infty} \frac{(-1)^n p^n e^{-np}}{b^{n+1}} \frac{[r-b(n+1)]^n}{\Gamma(n+1)} S_{b(n+1)}(r) \right]$$

and

$$S_k(t) = \begin{cases} 0 & 0 < t < k \\ 1 & t \geq k \end{cases}$$

is the unit step function.

In order to perform minimum error thresholding on a given image texture, it is necessary to know the prior probabilities of an edge point,

p_e, and of an interior point, p_i. An edge point is defined to be a point on the image line which is no more than a fixed distance d away from a true edge. We choose $d > 0$ so that $p_i \neq 0$. An interior point, as before, is a point that is at least distance k away from a true edge.

In the following we will consider, without loss of generality, only points within c_1-components. Given that a point is picked at random, let h be the probability density function for the distance y_1 to the next edge (the forward edge or edge on the right). From general results on random incidence into a renewal process we have [21]

$$h(y_1) = (1\text{-prob}[r \leq y_1])/E[r]$$

The function h is also the probability density function for the distance y_2 to the backward edge (the nearest edge on the left of the point). Then we have

$$h_j(y_1,y_2) = h(y_1)h_c(y_2/y_1)$$

where h_c is the conditional probability function for y_2 and h_j is the joint probability function for y_1 and y_2. If y_1 and y_2 are independent, then

$$h_j(y_1,y_2) = h(y_1)h(y_2)$$

From the above we now can derive expressions for the priors

$$p_i = \int_k^\infty \int_k^\infty h_j(y_1,y_2)dy_1dy_2$$

$$p_e = 1 - \int_d^\infty \int_d^\infty h_j(y_1,y_2)dy_1dy_2$$

For the discrete case we have

$$p_i = \sum_{y_1=k}^{\infty} \sum_{y_2=k}^{\infty} h(y_1,y_2)$$

$$p_e = 1 - \sum_{y_1=d+1} \sum_{y_2=d+1} h(y_1,y_2)$$

The set of interior points and the set of edge points are not complementary in the sense that they do not form a partition of the set of all points of the image line. Thus it is necessary that we normalize p_e and p_i.

$$p_e \leftarrow p_e/(p_e + p_i)$$

$$p_i \leftarrow p_i/(p_e + p_i)$$

Examples

1. Geometric distribution of component widths. Assume for simplicity that $b = 1$. Then

$$h(y_1) = (1-p)(1 - \sum_{y=1}^{y_1} (1-p)p^{y-1})$$

$$= (1-p) \sum_{y>y_1} (1-p)p^{y-1}$$

$$= (1-p)p^{y_1}$$

Thus

$$\text{Prob}[y_1 \geq k] = \sum_{y_1=k}^{\infty} (1-p)p^{y_1}$$

$$= p \sum_{y_1=k}^{\infty} (1-p)p^{y_1-1}$$

$$= p\,p^{k-1} = p^k$$

Since the geometric distribution is memoryless, y_1 and y_2 are independent random variables, and

$$p_i = \text{Prob}[y_1 \geq k,\ y_2 \geq k] = p^k p^k = p^{2k}$$

$$p_e = 1 - p^{2(d+1)}$$

Normalizing,

$$p_i = p^{2k}/(p^{2k} + 1 - p^{2(d+1)})$$

$$p_e = 1 - p_i$$

2. Exponential distribution of component widths. Let λ be the parameter of the distribution. Then

$$h(y_1) = \frac{1 - (1 - \text{Exp}(-\lambda y_1))}{1/\lambda} = \lambda\ \text{Exp}(-\lambda y_1)$$

$$\text{Prob}[y_1 \geq k] = \text{Exp}(-\lambda k)$$

The exponential distribution is also memoryless so that y_1 and y_2 are independent. We then have

$$p_i = \text{Exp}(-2\lambda k)$$

$$p_e = 1 - \text{Exp}(-2d\lambda)$$

Normalizing,

$$p_i = \text{Exp}(-2\lambda k)/(\text{Exp}(-2\lambda k) + 1 - \text{Exp}(-2d\lambda))$$

$$p_e = 1 - p_i$$

In order to use p_e, p_i and the expected values obtained above for minimum error edge detection, we will make the assumption that e_k is normally distributed at edge points as well as interior points. More precisely, we assume that e_k is $N(0,2v/k)$ at interior points and $N(E[e_k],Var[e_k])$ at edges. This assumption is certainly valid for interior points since, in this case, LS and RS are each the sum of k independent experimental values sampled from the same normal distribution. At edges, each of LS and RS is the sum of k_1 independent experimental values drawn from the normal distribution that represents one of the coloring processes and k_2 independent experimental values from the normal distribution that describes the other coloring process. The sum of k_1 and k_2 is k, but k_1 and k_2 will in general vary from point to point on the image line.

The assumption of normality of e_k at edges will hold well if the variances of k_1 and k_2 are low. This means that in the neighborhood of any edge point on the image line the number of pixels colored by either process remains almost constant. For example, this is trivially true for the constant distribution of cell widths, with $k \leq b$, b being the width of a cell. In this extreme case, $k_1 = k$ and $k_2 = 0$ or vice versa. However, if k_1 and k_2 have a high variance, then the normality assumption will not hold very well.

Thus, an important factor for the validity of the assumption is the variance of cell widths. Ideally, this variance should be small; however another property that would tend to make the assumption hold well is that the image model be more likely to contain cells whose widths are close to k. This will keep the probability that the neighborhoods C_ℓ and C_r extend

over more than one cell quite low.

Given the normality assumption, the following two step process can be used to compute an optimal k and t for a minimum error edge detector.

1) For a range of k, find the minimum error threshold for discriminating between edges and interior points. Since both e_k at edges and e_k at interior points are modeled by normal distributions with known parameters and priors, this is straightforward. Let er(k) be the probability of error for the minimum error threshold for e_k and let t(k) be the threshold.

2) Choose k such that $er(k) \leq er(k')$, for all k' considered. Then (k,t(k)) define the minimum error edge detector.

Figure 2 shows plots of er(k) as a function of k for the three cell width models presented in Section 2. Notice that the value of k which minimizes total errors is the mean cell width for all three models. The reason that the curves tend to level off at high k, rather than rise to a high error, is that as k becomes very large, the prior probability of interior points, p_i, approaches zero. For very high values of k, the near zero value of p_i causes the programs which compute minimum error thresholds to become unstable. Therefore, we arbitrarily stopped computing er(k) for $k > 20$. Figure 3a-e shows an example of the effect of k on the performance of e_k. Figure 3a contains a checkerboard texture with $b = 16$, $p = .5$, $m_1 = 30$, $m_2 = 20$, and $v_1 = v_2 = 10$. Figure 3b shows the true edges, while Figures 3c-e show the results of applying e_k, $k = 8$, 16 and 24, thresholding at the minimum error threshold for the appropriate k, and then performing non-maxima suppression across 8 pixels. Note that the results for the optimal value of k (16) are significantly better than choosing k too small (8) or too large (24).

5. Discussion

This paper has discussed the problem of detecting edges in cellular textures. A general edge detection procedure was proposed. This procedure involved applying an edge sensitive operator to the texture, and then thresholding the results of the edge operator and finally computing "peaks" from the above threshold points. This paper concentrated on the thresholding process and developed a minimum error thresholding procedure based on an analysis of the edge operator e_k. The thresholding procedure assumed that e_k was normally distributed at edges and at interior points.

The peak selection step was not considered in this paper. It is discussed in [20], which also includes examples of choosing optimal edge detectors for real textures, and a comparative classification study using optimal and suboptimal edge detectors.

References

1. N. Nahi and S. Lopez-Mora, "Estimation detection of object boundaries in noisy images," *IEEET-Automatic Control, 23,* 1978, 834-846.

2. J. Modestino and R. Fries, "Edge detection in noisy images using recursive digital filtering," *Computer Graphics and Image Processing, 6,* 1977, 409-433.

3. K. Shanmugan, F. Dickey and R. Dubes, "An optimal frequency domain filter for edge detection in digital pictures," *IEEET-Pattern Analysis and Machine Intelligence, 1,* 1979, 37-49.

4. D. Cooper and H. Elliot, "A maximum likelihood framework for boundary estimation in noisy images," Proc. IEEE Computer Society Conf. on Pattern Recognition and Image Processing, Chicago, IL, May 31-June 2, 1978, 25-31.

5. A. Rosenfeld and A. Kak, *Digital Picture Processing,* Academic Press, New York, 1976.

6. J. Weszka, C. Dyer and A. Rosenfeld, "A comparative study of texture features for terrain classification," *IEEET-Systems, Man and Cybernetics, 6,* 1976, 269-285.

7. D. Marr, "Early Processing of Visual Information," *Phil. Trans. Royal Society, B, 275,* 1976, 483-524.

8. L. Davis, S. Johns and J. K. Aggarwal, "Texture analysis using generalized cooccurrence matrices," *IEEET-Pattern Analysis and Machine Intelligence, 1,* 1979, 251-258.

9. L. Davis, M. Clearman and J. K. Aggarwal, "A comparative texture classification study based on generalized cooccurrence matrices," to appear in IEEE Conf. on Decision and Control, Miami, FL., Dec. 12-14, 1979.

10. N. Ahuja, "Mosaic models for image synthesis and analysis," Ph.D. dissertation, University of Maryland, Computer Science Dept., 1979.

11. B. Horn, "Understanding image intensities," *Artificial Intelligence, 8,* 1977, 208-231.

12. B. McCormick and S. Jayaramamurthy, "Time series models for texture synthesis," *J. Computer and Information Sciences, 3,* 1974, 329-343.

13. J. Tou, D. Kao and Y. Chang, "Pictorial texture analysis and synthesis," Proc. Third Int. Joint Conf. on Pattern Recognition, Coronado CA., Nov. 8-11, 1976, 590.

14. E. Wong, "Two-dimensional random fields and representations of images," *SIAM J. Applied Math., 16,* 1968, 756-770.

15. W. Pratt and O. Faugeras, "Development and evaluation of stochastic-based visual texture fields," Proc. 4th Int. Joint Conf. on Pattern Recognition, Nov. 1978, 545-548.

16. M. Hassner and J. Sklansky, "Markov random fields of digitized image texture," Proc. 4th Int. Joint Conf. on Pattern Recognition, Nov. 1978, 538-540.

17. K. Abend, I. Harley and L. Kanal, "Classification of binary random patterns," *IEEET-Information Theory, 11,* 1965, 538-544.

18. M. Duff, "CLIP-4: A large scale integrated circuit array parallel processor," Proc. 3rd Int. Joint Conf. on Pattern Recognition, 1976, 728-732.

19. B. Kruse, "A parallel picture processing machine," *IEEET-Computers, 22,* 1973, 1075-1087.

20. L. Davis and A. Mitiche, "Optimal texture edge detection procedures," in preparation.

21. A. Drake, *Fundamentals of Applied Probability Theory,* McGraw-Hill, New York, 1967.

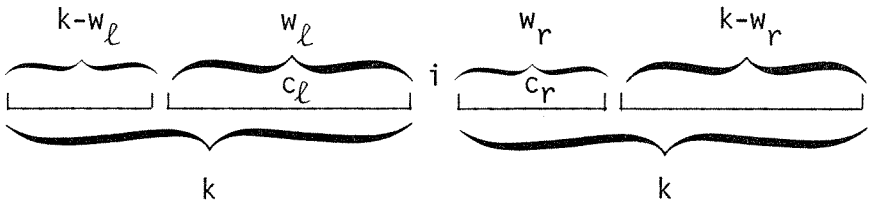

Figure 1. Neighborhood of an edge point, i.

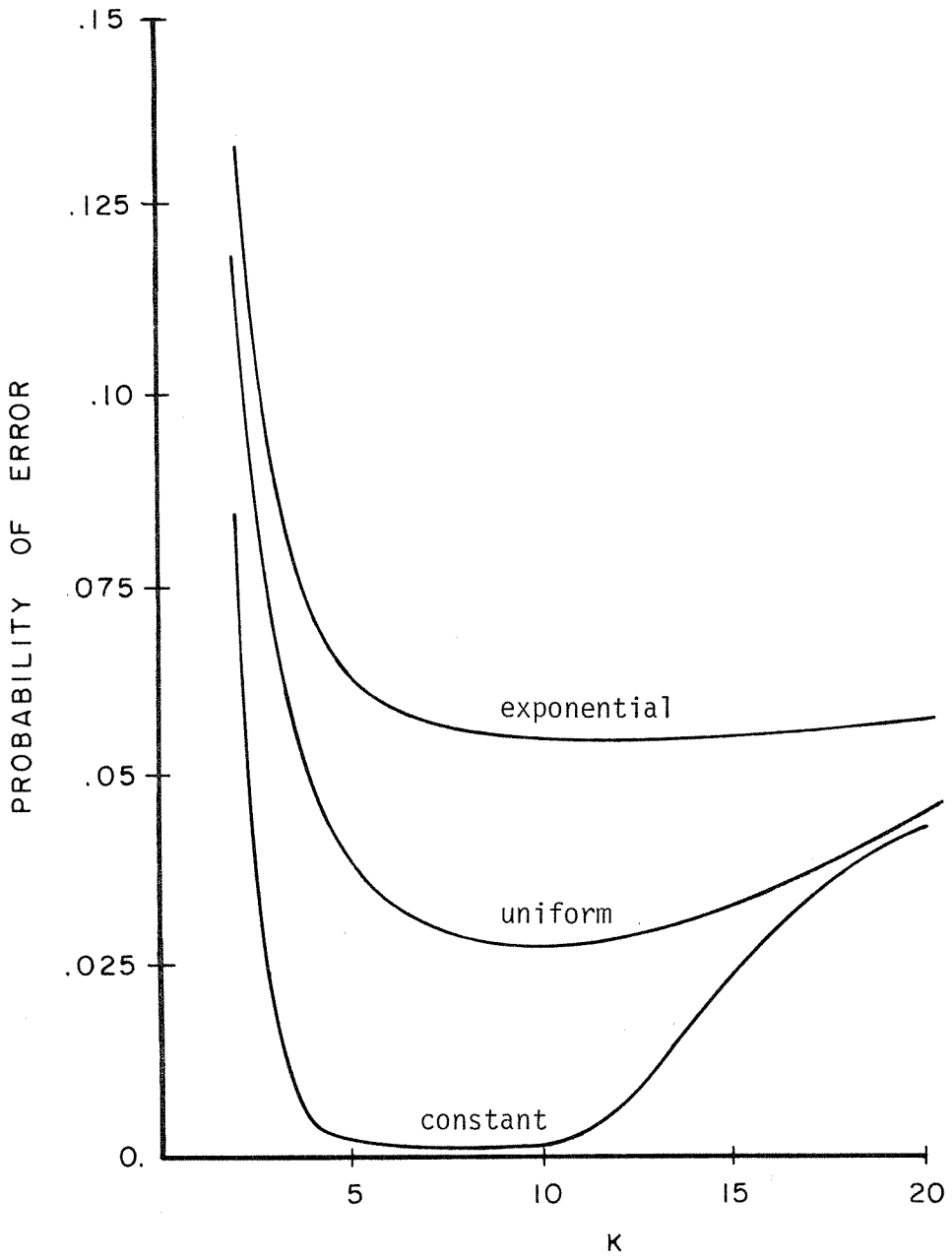

Figure 2. Plots of er(k) as a function of k for the three cell width models. All parameters are the same for all three models: $m_1 = 10$, $m_2 = 5$, $v_1 = v_2 = 2$, $p = .5$ and $w_0 = 10$.

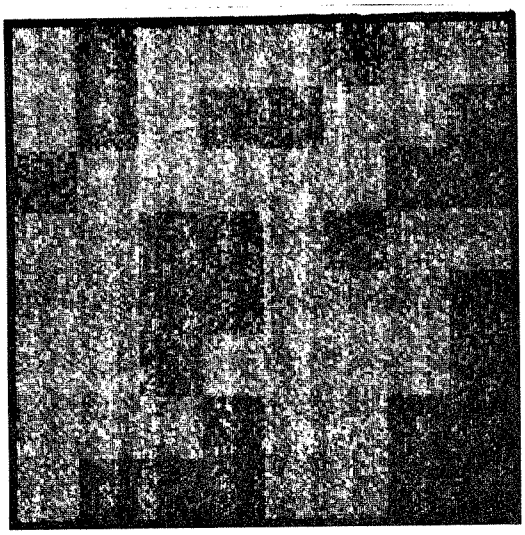

a) original texture

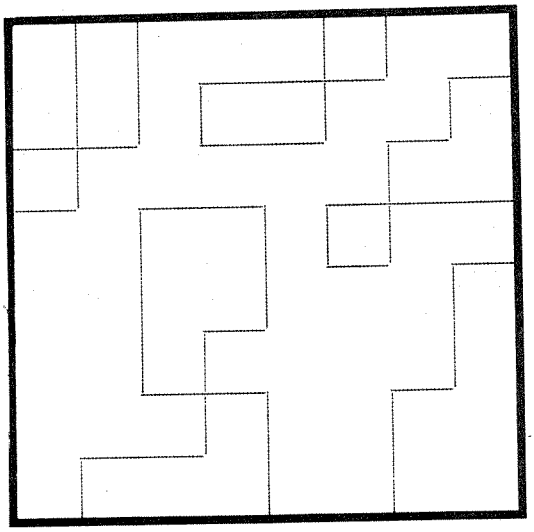

b) true edges

Figure 3. Application of e_k to a checkerboard texture.

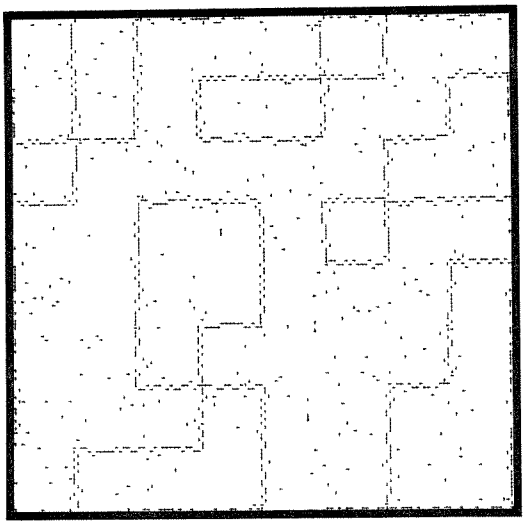

c) k = 8

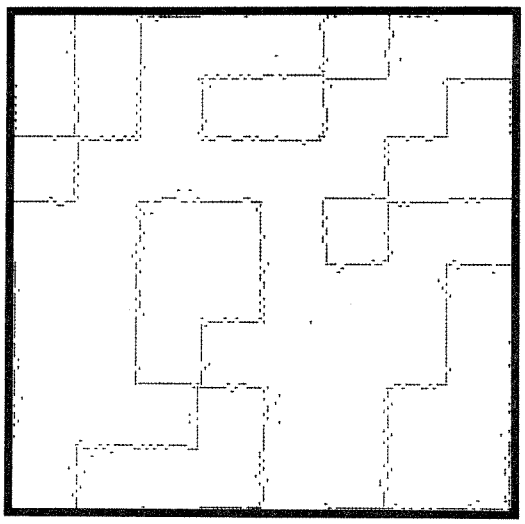

d) k = 16

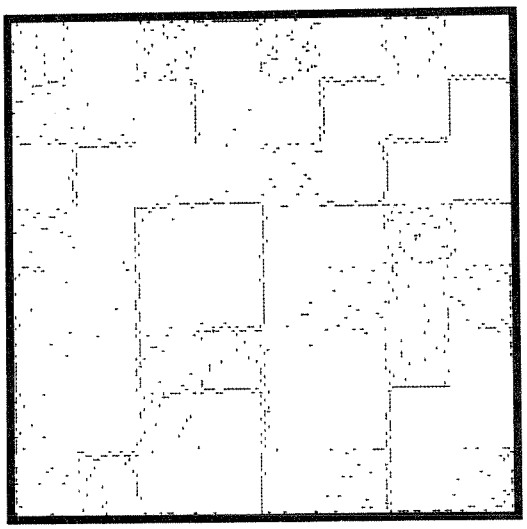

e) k = 24

Figure 3. continued.